

Spherical top-hat Collapse of a Viscous Unified Dark Fluid

Wei Li^{1,2*} and Lixin Xu²

¹*Department of Physics, Bohai University, Jinzhou, 121013, China and*

²*Institute of Theoretical Physics, Dalian University of Technology, Dalian, 116024, P.R.China*

In this paper, we test the spherical collapse of a viscous unified dark fluid (VUDF) which has constant adiabatic sound speed and show the nonlinear collapse for VUDF and baryons which are important to form the large scale structure of our Universe. By varying the values of model parameters α and ζ_0 , we discuss their effects on the nonlinear collapse of the VUDF model. The analyzed results show that, within the spherical top-hat collapse framework, larger values of α and smaller values of ζ_0 make the structure formation earlier and faster.

PACS numbers: 98.80.-k, 95.35.+d, 95.36.+x

Keywords: Viscous unified dark fluid, spherical collapse, top-hat profile

I. INTRODUCTION

As an competitive model to explain the lately accelerated expansion of universe, a unified dark fluid (UDF) model [1–3, 5–8][10, 11] was investigated extensively in the recent years. The striking features of the UDF model are that it combines cold dark matter and dark energy and that it behaves like the cold dark matter and the dark energy at the early epoch and the late time respectively. Furthermore, it can match the image of the Λ CDM model very well on the background level. Among those UDF models, one same assumption that the medium of universe is modeled as an idealized perfect fluid were taken, which means that all components of the matter-energy in our universe are considered as a perfect fluid without viscosity. However, in the recently years, more and more cosmological observations suggest that our universe is permeated by imperfect fluid, in which the negative pressure, as was argued in [12], [13], an effective pressure including bulk viscosity can drive the present acceleration of universe. The first attempts at creating a viscosity theory of relativistic fluids were executed by Eckart [14] and Landau and Lifshitz [15] who considered only first-order deviation from equilibrium. The general form of the bulk viscosity is chosen as a time-dependent function or a density-dependent function. In some literature, a density-dependent viscosity $\zeta = \zeta_0 \rho^m$ coefficient is widely investigated, where the condition $\zeta_0 > 0$ ensures a positive entropy production in conformity with the second law of thermodynamics. For simplification, we will devote ourselves to studying the case $m = \frac{1}{2}$, which the similar form being taken in the Ref. [11][22–24]

For any proposed cosmological model, if it's cosmic observations cannot coincide with the theoretical calculation, it would be ruled out, so does the VUDF model. As the large-scale structure formation originates from the primordial quantum perturbations of our universe, the non-linear stages of perturbations become very important

during one investigating the evolutions of density perturbations of VUDF model. A fully nonlinear analysis is a cumbersome task usually handled by hydrodynamical/N-body numerical codes (see, e.g., [16–19]). However, to best of our knowledge, the hydrodynamical/N-body numerical simulation is very implicated and expensive.

In this paper we focus on the collapse of a spherically symmetric perturbation of VUDF model, with a classical top-hat profile, instead of using the cumbersome hydrodynamical/N-body numerical simulation. We modify the pressure of UDF $p = \alpha\rho - A$ in the Ref.[3] into the form $p = \alpha\rho - \zeta_0\rho - A$ to obtain the VUDF model. As mentioned in the Ref. [4], one need to avoid the averaging problem [20] when studying the non-linear perturbations. The problem comes from the fact that

$$\langle p \rangle = -\langle A/\rho^\beta \rangle \neq -A/\langle \rho \rangle^\beta = p(\langle \rho \rangle), \quad (1)$$

in the case of $\beta \neq 0$. However, for a model with a linear relation $p = \alpha\rho - \zeta_0\rho - A$, it is not the problem. So it would be interesting to study the evolution of non-linear perturbation in this VUDF model because of escaping from the averaging problem. Avoid using the hydrodynamical/N-body numerical simulation, we will research the large structure formation in the framework of spherical top-hat collapse for the viscous unified dark fluid (VUDF).

The paper is organized as follows. In section II, a brief introduction of the VUDF with a constant adiabatic sound speed is given. Then, we present some basic equations for spherical top-hat collapse of viscous fluid in section III. The method and main results are summarized in section IV. The last section is the conclusion.

II. VISCOUS UNIFIED DARK FLUID WITH CONSTANT ADIABATIC SOUND SPEED

In this section, we will give some basic equations of a VUDF model which has a constant adiabatic sound speed (CASS). In order to obtain the viscous unified dark fluid, we rewrite the pressure of UDF $p = \alpha\rho - A$ in the Ref.[3]

*corresponding author: liweizhd@126.com

into the form

$$p_d = p - 3H\zeta, \quad (2)$$

this expression includes the UDF model as its special case when $\zeta = 0$, as for the case that $\zeta \neq 0$, when adopting the normal form $\zeta = \frac{\zeta_0}{\sqrt{3}}\rho^{\frac{1}{2}}$ which the similar form being taken in the Ref.[11],[22–24], we have the pressure of VUDF

$$p_d = \alpha\rho_d - \zeta_0\rho_d - A, \quad (3)$$

where $A = \rho_{d0}(1 + \alpha - \zeta_0)(1 - B_s)$. Applying the energy conservation of VUDF, one can deduce its energy density as the following form

$$\rho_d = \rho_{d0} \left\{ (1 - B_s) + B_s a^{-3(1+\alpha-\zeta_0)} \right\}, \quad (4)$$

where the model parameters B_s , α , and ζ_0 are all in the range $[0, 1]$. So one obtains the equation of state (EoS)

$$w_d = \frac{p_d}{\rho_d} = \alpha - \zeta_0 - \frac{(1 + \alpha - \zeta_0)(1 - B_s)}{(1 - B_s) + B_s a^{-3(1+\alpha-\zeta_0)}}, \quad (5)$$

and adiabatic sound speed

$$c_s^2 = \left(\frac{\partial p_d}{\partial \rho_d} \right)_s = \frac{dp_d}{d\rho_d} = \rho_d \frac{dw_d}{d\rho_d} + w_d = \alpha - \zeta_0, \quad (6)$$

where A , ζ_0 and w_d are the integration constant, bulk viscosity coefficient and the equation of state (EoS) of VUDF respectively. Therefore, the Friedmann equation in a spatially flat FRW universe is given as

$$H^2 = H_0^2 \left\{ (1 - \Omega_b - \Omega_r) \left[(1 - B_s) + B_s a^{-3(1+\alpha-\zeta_0)} \right] + \Omega_b a^{-3} + \Omega_r a^{-4} \right\}, \quad (7)$$

where H is the Hubble parameter and $H_0 = 100 h \text{ km s}^{-1} \text{ Mpc}^{-1}$ is its present value, and Ω_i ($i = b, r$) are dimensionless energy density parameters, where b and r stand for baryon and radiation separately.

III. EQUATIONS OF SPHERICAL TOP-HAT COLLAPSE OF VISCOUS FLUID

The spherical collapse (SC) as a simple analytical model was first introduced by Gunn and Gutt 1972 [21] in order to calculate the evolution of perturbations in falling material into a bound system which provides a way to glimpse into the nonlinear regime of perturbation theory. Usually, the SC model is used to investigate a spherically symmetric perturbation which embedded in a static, expanding or collapsing homogeneous background. In this paper we focus on the collapse of a spherically symmetric perturbation in a homogenous expanding background, with a classical top-hat profile which has the constant density [25] in the perturbed region. With the assumption of a top-hat profile, one maintains the

simplified spherical collapse model as the uniformity of the perturbation throughout the collapse, which making its evolution only time-dependent. So we do not need to worry about the gradients through the collapse.

In the spherical top-hat collapse (SC-TH) model, the background evolution equations are still in the following forms

$$\dot{\rho} = -3H(\rho + p), \quad (8)$$

$$\frac{\ddot{a}}{a} = -\frac{4\pi G}{3} \sum_i (\rho_i + 3p_i), \quad (9)$$

where $H = \dot{a}/a$ is the Hubble parameter. For the perturbed region, the basic equations which depend on local quantities can be written as

$$\dot{\rho}_c = -3h(\rho_c + p_c), \quad (10)$$

$$\frac{\ddot{r}}{r} = -\frac{4\pi G}{3} \sum_i (\rho_{ci} + 3p_{ci}). \quad (11)$$

Here the perturbed quantities ρ_c and p_c are defined as $\rho_c = \rho + \delta\rho$, $p_c = p + \delta p$; and $h = \dot{r}/r$ and r are the local expansion rate and the local scale factor respectively, and furthermore h relates to local expansion rate in the STHC model by [26, 27]

$$h = H + \frac{\theta}{3a}, \quad (12)$$

where $\theta \equiv \nabla \cdot \vec{v}$ is the divergence of the peculiar velocity.

So, the equations of density contrast $\delta_i = (\delta\rho/\rho)_i$ and θ are: [25, 26]

$$\dot{\delta}_i = -3H(c_{e_i}^2 - w_i)\delta_i - [1 + w_i + (1 + c_{e_i}^2)\delta_i] \frac{\theta}{a}, \quad (13)$$

$$\dot{\theta} = -H\theta - \frac{\theta^2}{3a} - 4\pi G a \sum_i \rho_i \delta_i (1 + 3c_{e_i}^2), \quad (14)$$

where the effective sound speed is $c_{e_i}^2 = (\delta p/\delta\rho)_i$, where i stands for different energy component. The Eq. (13) and Eq. (14) can be rewritten into the form in regard to the scale factor a

$$\delta'_i = -\frac{3}{a}(c_{e_i}^2 - w_i)\delta_i - [1 + w_i + (1 + c_{e_i}^2)\delta_i] \frac{\theta}{a^2 H}, \quad (15)$$

$$\theta' = -\frac{\theta}{a} - \frac{\theta^2}{3a^2 H} - \frac{3H}{2} \sum_i \Omega_i \delta_i (1 + 3c_{e_i}^2), \quad (16)$$

where we have used the definition $\Omega_i = 8\pi G \rho_i / 3H^2$.

From the above equations, one can find that the w_c and c_e^2 are important quantities. The definition of the EoS w_c [25] is:

$$w_c = \frac{p + \delta p}{\rho + \delta\rho} = \frac{w}{1 + \delta} + c_e^2 \frac{\delta}{1 + \delta}. \quad (17)$$

The effective sound speed c_e^2 of the CASS model is given as

$$c_e^2 = \frac{\delta p}{\delta\rho} = \frac{p_c - p}{\rho_c - \rho}. \quad (18)$$

So, substituting the relation $p = \alpha\rho - \zeta_0\rho - A$ into the above equation, one has

$$c_e^2 = \frac{[(\alpha - \zeta_0)\rho_c] - A - [(\alpha - \zeta_0)\rho - A]}{\rho_c - \rho} = \alpha - \zeta_0 \quad (19)$$

IV. THE METHOD AND RESULTS

In this section, we will use the spherical collapse model to investigate the non-linear evolution of the VUDF perturbations. As the baryon and VUDF are the possible components that forming the large scale structure, we will just consider the two components, where the results of some model parameters are come from the Ref. [3]: $\Omega_d = 0.956$, $H_0 = 71.341\text{km s}^{-1}\text{Mpc}^{-1}$, and $\Omega_b = 0.044$. With the aid of using the software **Mathematica** and setting the initial conditions (ICs) δ_d and δ_b at the redshift $z = 1000$ in Ref. [25], we solve the differential equations of perturbations.

In order to explore the influences of α on the spherical collapse of baryon and unified dark fluid, we immobilize $\delta_d(z = 1000) = 3.5 \times 10^{-3}$, $\delta_b(z = 1000) = 10^{-5}$, $\zeta_0 = 0$, and $B_s = 0.229$, but change the model parameter $\alpha = 0, 10^{-3}, 10^{-2}$, and 10^{-1} respectively. We obtain the same calculated results as Table I in the Ref. [9], where the redshift z_{ta} is on behalf of the turnaround redshift when the collapse is beginning. From Table I, one can conclude that the perturbations collapse earlier and faster for the larger values of α and larger values of $c_e^2 = \alpha$.

Model	α	z_{ta}	$\delta_b(z_{ta})/\delta_d(z_{ta})$
a	0	0.0678	1.240
b	10^{-3}	0.111	1.211
c	10^{-2}	0.138	0.689
d	10^{-1}	0.940	0.010

TABLE I: Models for the STHC model, where the values of α are small positive values due to the constraint from background evolution history. The redshift z_{ta} denotes the turnaround redshift when the perturbed region begin to collapse.

In the following, we will show the influence of bulk viscosity coefficient ζ_0 on the evolution of the density perturbations of baryon and VUDF. Here we alter the values of ζ_0 for the different models which fix $\alpha = 10^{-1}, 10^{-2}, 10^{-3}$, and 0 respectively. The corresponding evolutions of density perturbations are shown in Figure 1, 2, 3, 4. From these four figures, one can see that the higher value of α is taken, the more obvious influence on the collapse is gained. On the contrary, smaller value of α can result in unobvious effect, for example in the Figure 4, when $\alpha = 0$, one almost unable to distinguish that four curves. Seeing from the Figure 1-4, the horizon line denotes the limit of linear perturbation, i.e.

$\delta = 1$ and the vertical parts of the curved lines denote the collapse of the perturbed regions, therefore, one can see that smaller value of bulk viscosity coefficient ζ_0 can result in earlier collapse, that is to say, larger value of bulk viscosity coefficient ζ_0 can make the collapse more later, these results are compatible with the well-known convention that the value of bulk viscosity coefficient ζ_0 should be not too large.

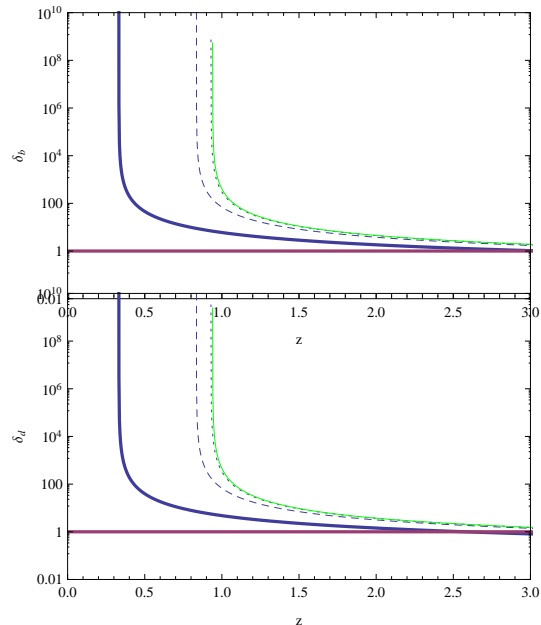


FIG. 1: The evolutions of density perturbations with respect to the redshift for the models $\alpha = 10^{-1}$. The top and bottom panels are for baryons and VUDF respectively. Where the thick, dashed, dotted and solid curved lines are for the models $\zeta_0 = 10^{-1}, 10^{-2}, 10^{-3}, 0$ respectively. The horizon line denotes the limit of linear perturbation, i.e. $\delta = 1$. The vertical parts of the curved lines denote the collapse of the perturbed regions.

It's time to show the influence of ζ_0 on the evolution of the equation of state (EoS) of the VUDF w_d and the EoS of the collapse region w_c . Observing the evolving curves of w_c in the Figure 5-8, one can easily conclude that higher values of ζ_0 result in values of w_c closer and higher to $w_c = 0$ during the collapse as shown in Figure 5 and 6, and result in values of w_c closer and lower to $w_c = 0$ during the collapse as shown in Figure 7, but result in values of w_c almost overlapping together as shown in Figure 8. However, the effects of ζ_0 on the evolution of the equation w_d is very different comparing to the results

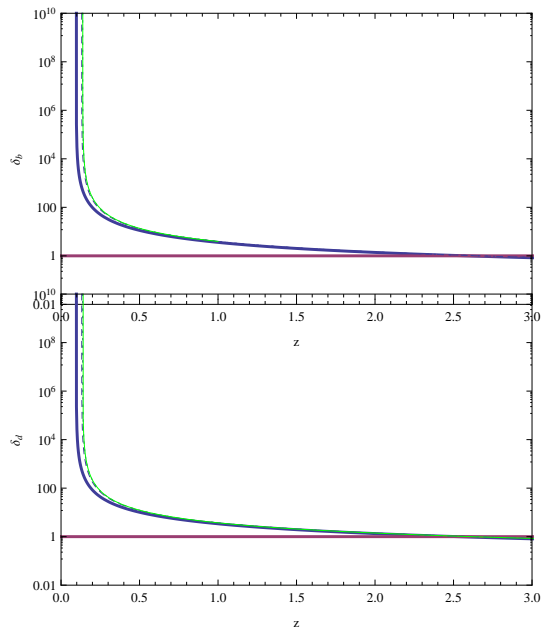


FIG. 2: The evolutions of density perturbations with respect to the redshift for the models $\alpha = 10^{-2}$. The top and bottom panels are for baryons and VUDF respectively. Where the thick, dashed, dotted and solid curved lines are for the models $\zeta_0 = 10^{-2}, 10^{-3}, 10^{-4}, 0$ respectively. The horizon line denotes the limit of linear perturbation, i.e. $\delta = 1$. The vertical parts of the curved lines denote the collapse of the perturbed regions.

above. Apart from the almost distinguishable influence of ζ_0 on w_d as shown in Figure 6-8, we know that smaller ζ_0 make the curves of w_d higher as shown in Figure 5. Base on the discussion above, we can draw a conclusion that the influence of ζ_0 on the evolution of w_d and w_c are enhanced as increasing the values of α .

Through the calculation and analysis above, for the VUDF model, it is possible to format the large scale structure. Also, it is obvious that the model parameters ζ_0 and α have influence on the density perturbations evolutions.

V. CONCLUSION

In this paper, we investigated the density perturbations of a VUDF model with a constant adiabatic sound

speed in the framework of spherical top-hat collapse, the results show that it is possible to form large scale structure in the VUDF model. We study their influence on

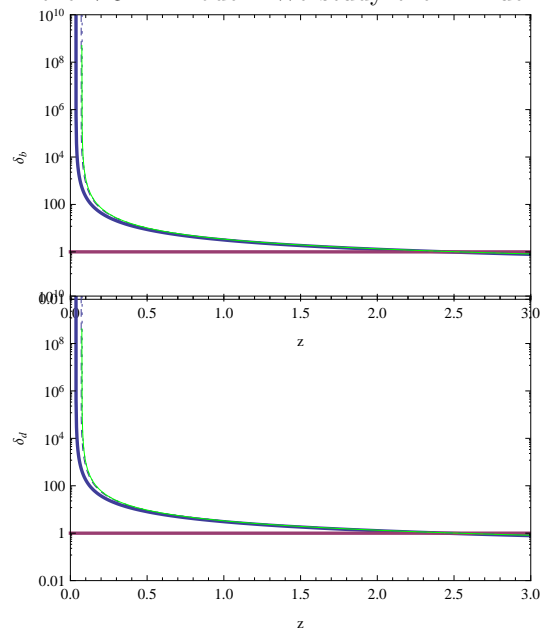


FIG. 3: The evolutions of density perturbations with respect to the redshift for the models $\alpha = 10^{-3}$. The top and bottom panels are for baryons and VUDF respectively. Where the thick, dashed, dotted and solid curved lines are for the models $\zeta_0 = 10^{-2}, 10^{-3}, 10^{-4}, 0$ respectively. The horizon line denotes the limit of linear perturbation, i.e. $\delta = 1$. The vertical parts of the curved lines denote the collapse of the perturbed regions.

the evolutions of perturbation through varying the values of ζ_0 and α . Through the calculation and analysis, we concluded that smaller values of ζ_0 and larger values of α can make the density perturbations collapse earlier and faster, and furthermore we can also conclude that the influence of ζ_0 on the evolution of w_d and w_c are enhanced as increasing the values of α . In the following work, we will try to apply the spherical collapse to other cosmological models and compare the simulated results with the observed large scale structure of universe.

VI. ACKNOWLEDGEMENTS

L. Xu's work is supported in part by NSFC under the Grants No. 11275035 and "the Fundamental Research Funds for the Central Universities" under the Grants No. DUT13LK01.

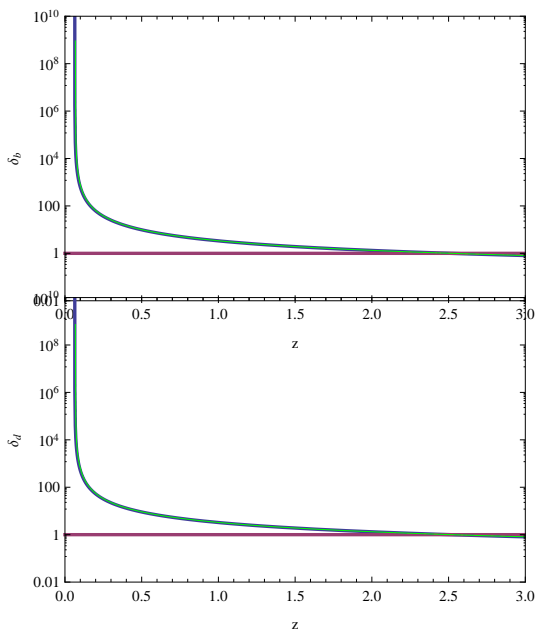


FIG. 4: The evolutions of density perturbations with respect to the redshift for the models $\alpha = 0$. The top and bottom panels are for baryons and VUDF respectively. Where the thick, dashed, dotted and solid curved lines are for the models $\zeta_0 = 10^{-3}, 10^{-4}, 10^{-5}, 0$ respectively. The horizon line denotes the limit of linear perturbation, i.e. $\delta = 1$. The vertical parts of the curved lines denote the collapse of the perturbed regions.

-
- [1] W. Hu and D. J. Eisenstein, Phys. Rev. D 59, 083509(1999); H. Velten, D. J. Schwarz, JCAP 1109, 016 (2011); W.S. Hipolito-Ricaldi, H.E.S. Velten, W. Zimdahl, Phys. Rev. D 82 063507(2010).
- [2] K. N. Ananda and M. Bruni, Phys. Rev. D. 74, 023523 (2006), arXiv:astro-ph/0512224; A. Balbi, M. Bruni, C. Quercellini, Phys. Rev. D 76, 103519 (2007).
- [3] L. Xu, Y. Wang, H. Noh, Phys. Rev. D 85, 043003 (2012) [arXiv:1112.3701].
- [4] L. Xu, Eur. Phys. J. C (2013) 73:2344, DOI: 10.1140/epjc/s10052-013-2344-7, arXiv:1302.6637 [astro-ph.CO]
- [5] A.Y. Kamenshchik, U. Moschella and V. Pasquier, 2001 Phys. Lett. B 511 265.
- [6] T. Barreiro, O. Bertolami and P. Torres, 2008 Phys. Rev. D 78 043530;
- [7] J. Lu, Y. Gui, L. Xu, Eur. Phys. J. C 63,349(2009); N. Liang, L. Xu, Z. H. Zhu, Astrono. & Astrophys, 527, A11(2011); Z. Li, P. Wu, H. Yu, JCAP09,017(2009); P. Wu, H. Yu, Phys. Lett. B 644,16(2007);
- [8] L. Xu, J. Lu, Y. Wang, Eur. Phys. J. C 72 1883 (2012).
- [9] L. Xu, Eur. Phys. J. C (2013) 73:2344. arXiv:1302.6637 [astro-ph.CO].
- [10] L. Xu, arXiv:1210.5327 [astro-ph.CO].
- [11] Wei Li, Lixin Xu Viscous generalized Chaplygin gas as a unified dark fluid, Eur. Phys. J. C (2013) 73:2471 DOI 10.1140/epjc/s10052-013-2471-1
- [12] [16] A. B. Balakin, D. Pavon, D. J. Schwarz, and W. Zimdahl, New J. Phys. 5, 85 (2003).
- [13] W. Zimdahl, D. J. Schwarz, A. B. Balakin, and D. Pavon, Phys. Rev. D 64, 063501 (2001).
- [14] C. Eckart, Phys. Rev. 58, 919 (1940)
- [15] L.D. Landau, E.M. Lifshitz, Fluid Mechanics (Butterworth Heinemann, Oxford, 1987)
- [16] A.V. Maccio', C. Quercellini, R. Mainini, L. Amendola, and S. A. Bonometto, Phys. Rev. D 69, 123516 (2004).
- [17] N. Aghanim, A. C. da Silva, and N. J. Nunes, Astron. Astrophys. 496, 637 (2009).
- [18] M. Baldi, V. Pettorino, G. Robbers, and V. Springel, Mon. Not. R. Astron. Soc. 403, 1684 (2010).
- [19] B. Li, D. F. Mota, and J. D. Barrow, Astrophys. J. 728, 109 (2011).
- [20] L.M.G. Beca, P.P. Avelino, Mon. Not. Roy. Astron. Soc. 376,1169(2007); P. P. Avelino, L. M. G. Beça, C. J. A. P. Martins, Phys. Rev. D 77, 063515 (2008).
- [21] J. E. Gunn, J. R. Gott, ApJ, 176 (1972) 1.
- [22] C.J. Feng, X.Z. Li, X.Y. Shen, arXiv:1202.0058v1 [astro-ph.CO]
- [23] C.J. Feng, X.Z. Li, Phys. Lett. B 680, 355 (2009). arXiv:0905.0527 [astro-ph.CO]
- [24] X.H. Zhai, Y.D. Xu, X.Z. Li, Int. J. Mod. Phys. D 15, 1151 (2006). arXiv:astro-ph/0511814
- [25] R. A. A. Fernandes, et al, Phys. Rev. D.85 083501,(2012).
- [26] L. R. Abramo, R. C. Batista, L. Liberato, and R. Rosen-

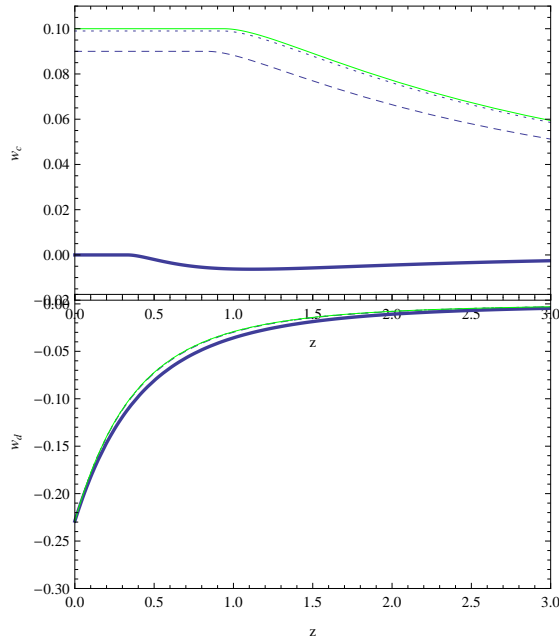


FIG. 5: The evolutions of w_c and w_d with respect to the redshift z for different models $\alpha = 10^{-1}$. The top and bottom panels are for w_c and w_d respectively. Where the thick, dashed, dotted and solid curved lines are for $\zeta_0 = 10^{-1}, 10^{-2}, 10^{-3}, 0$ respectively.

- feld, Phys. Rev. D. 79, 023516 (2009).
 [27] R. A. A. Fernandes, J. P. M. de Carvalho, and A.Yu. Kamenshchik, etc. Phys. Rev. D. 85, 083501 (2012).

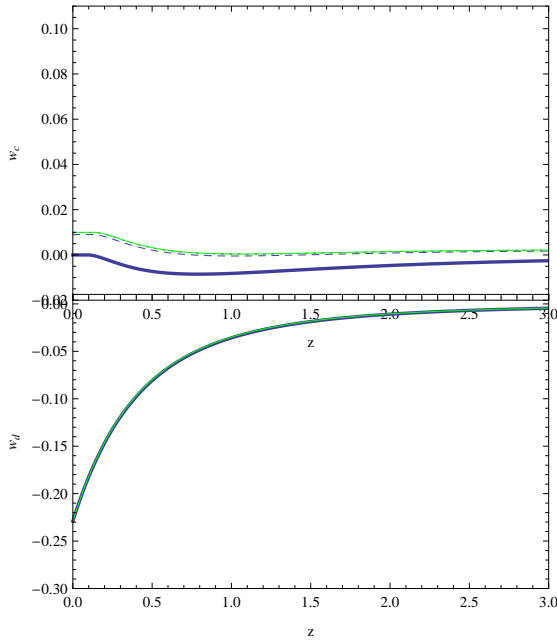


FIG. 6: The evolutions of w_c and w_d with respect to the redshift z for different models $\alpha = 10^{-2}$. The top and bottom panels are for w_c and w_d respectively. Where the thick, dashed, dotted and solid curved lines are for $\zeta_0 = 10^{-2}, 10^{-3}, 10^{-4}, 0$ respectively.

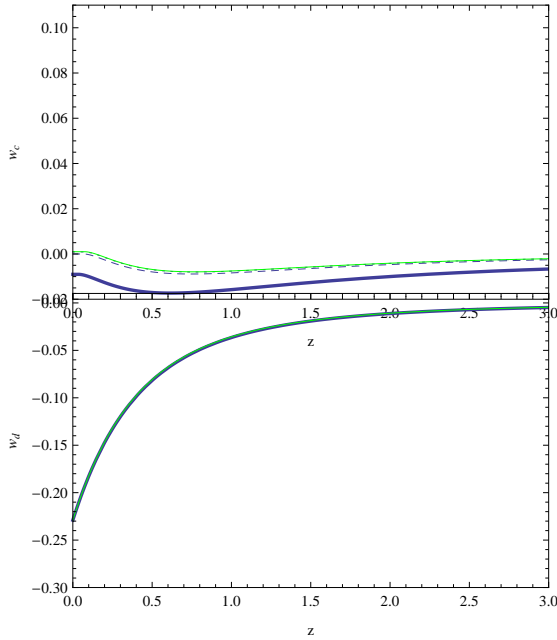


FIG. 7: The evolutions of w_c and w_d with respect to the redshift z for different models $\alpha = 10^{-3}$. The top and bottom panels are for w_c and w_d respectively. Where the thick, dashed, dotted and solid curved lines are for $\zeta_0 = 10^{-2}, 10^{-3}, 10^{-4}, 0$ respectively.

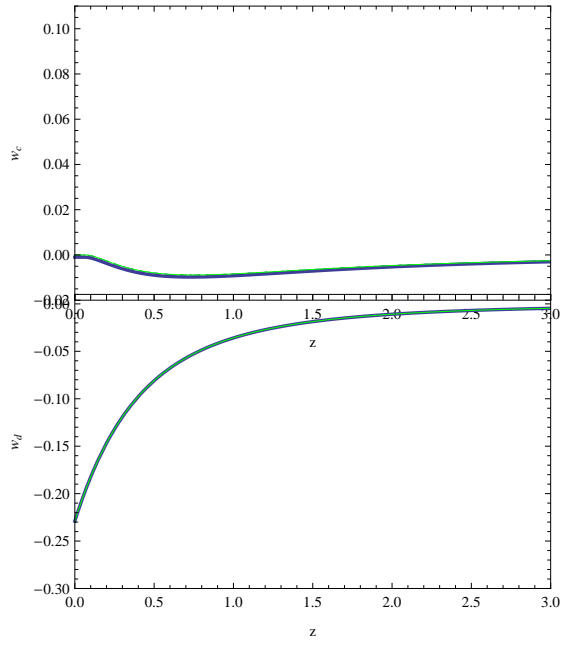


FIG. 8: The evolutions of w_c and w_d with respect to the redshift z for different models $\alpha = 0$. The top and bottom panels are for w_c and w_d respectively. Where the thick, dashed, dotted and solid curved lines are for $\zeta_0 = 10^{-3}, 10^{-4}, 10^{-5}, 0$ respectively.